DISCOVERING BUGS IN VISION MODELS USING OFF-THE-SHELF IMAGE GENERATION AND CAPTIONING

Anonymous authors
Paper under double-blind review

ABSTRACT

Automatically discovering failures in vision models under real-world settings remains an open challenge. This work shows how off-the-shelf, large-scale, image-to-text and text-to-image models, trained on vast amounts of data, can be leveraged to automatically find such failures. In essence, a conditional text-to-image generative model is used to generate large amounts of synthetic, yet realistic, inputs given a ground-truth label. A captioning model is used to describe misclassified inputs. Descriptions are used in turn to generate more inputs, thereby assessing whether specific descriptions induce more failures than expected. As failures are grounded to natural language, we automatically obtain a high-level, human-interpretable explanation of each failure. We use this pipeline to demonstrate that we can effectively interrogate classifiers trained on IMAGENET to find specific failure cases and discover spurious correlations. We also show that we can scale the approach to generate adversarial datasets targeting specific classifier architectures. This work demonstrates the utility of large-scale generative models to automatically discover bugs in vision models in an open-ended manner. We also describe a number of limitations and pitfalls related to this approach.

1 INTRODUCTION

Deep learning has enabled breakthroughs in a wide variety of fields (Goodfellow et al., 2016; Krizhevsky et al., 2012; Hinton et al., 2012), and deep neural networks are ubiquitous in many applications, including autonomous driving (Bojarski et al., 2016) and medical imaging (De Fauw et al., 2018). Unfortunately, these models are known to exhibit numerous failures arising from using *shortcuts* and *spurious correlations* (Geirhos et al., 2020a; Arjovsky et al., 2019; Torralba et al., 2011; Kuehlkamp et al., 2017). As a result, they can fail catastrophically when training and deployment data differ (Buolamwini & Gebru, 2018). Hence, it is important to ensure that models are robust and generalize to new deployment settings.

Yet, only a few tools exist to automatically find failure cases on unseen data. Some methods analyze the performance of models by collecting new datasets (usually by scraping the web). These datasets must be large enough to obtain some indication of how models perform on a particular subset of inputs (Hendrycks et al., 2019; 2020; Recht et al., 2019). Other methods rely on expertly crafted, synthetic (and often unrealistic) datasets that highlight particular shortcomings (Geirhos et al., 2022; Xiao et al., 2020).

In this work, we present a methodology to automatically find failure cases of image classifiers in an open-ended manner, without prior assumptions on the types of failures and how they arise. We leverage off-the-shelf, large-scale, text-to-image, generative models, such as DALL·E 2 (Ramesh et al., 2022), IMAGEN (Saharia et al., 2022) or STABLE-DIFFUSION (Rombach et al., 2022), to obtain realistic images that can be reliably manipulated using the text prompt. We also leverage captioning models, such as FLAMINGO (Alayrac et al., 2022) or LEMON (Hu et al., 2021), to retrieve human-interpretable descriptions of each failure case. This provides the following advantages: *(i)* generative models trained on web-scale datasets can be re-used and have broad non-domain-specific coverage; *(ii)* they demonstrate basic compositionality, can generate novel data and can faithfully capture the essence of (most) prompts, thereby allowing images to be realistically manipulated; *(iii)* textual descriptions of failures can be easily interpreted (even by non-experts) and interrogated (e.g., by performing counterfactual analyses). Overall, our contributions are as follows:

- We describe a methodology to discover failures of image classifiers trained on IMAGENET (Deng et al., 2009). To the contrary of prior work, we leverage off-the-shelf generative models, thereby avoiding the need to collect new datasets or to rely on manually crafted synthetic images.
- Our approach surfaces failures that are human-interpretable by clustering and captioning inputs on which classifiers fail. These captions can be modified to produce alternative hypotheses of why failures occur allowing insights into the limitations of a given model.
- We demonstrate the scalability of the approach by generating adversarial datasets (akin to IMAGENET-A; Hendrycks et al., 2019). In contrast to IMAGENET-A, our new generated datasets align more closely with the original training distribution from IMAGENET and generalize to multiple classifier architectures.

Importantly, while this work focuses on vision models trained on IMAGENET, it is neither limited to IMAGENET nor the visual domain. It serves as a **proof-of-concept** that demonstrates how large-scale, off-the-shelf, generative models (Bommasani et al., 2021) can be combined to automate the discovery of *bugs* in machine learning models and produce compelling, interpretable descriptions of model failures. The approach is agnostic to the model architecture, which can be treated as a black box.

2 RELATED WORK

Model failures. Spurious correlations can entice models to learn unintended shortcuts that obtain high accuracy on the training set but fail to generalize (Lapuschkin et al., 2019; Geirhos et al., 2020a). Recht et al. (2019) show that the accuracy of IMAGENET models is impacted by changes in the data collection process, while Torralba et al. (2011); Khosla et al. (2012); Choi et al. (2012) explore how contextual bias affects generalization. Mania et al. (2019) demonstrate that models trained on IMAGENET make consistent mistakes with one another and Geirhos et al. (2020b) show that these mistakes are not necessarily consistent with human judgment.

Evaluation datasets. Understanding how model failures arise and empirically analyzing their consequences often requires collecting and annotating new test datasets. Hendrycks et al. (2019) collected datasets of natural adversarial examples (IMAGENET-A and IMAGENET-O) to evaluate how model performance degrades when inputs have limited spurious cues. Hendrycks et al. (2020) collected four real-world datasets (including IMAGENET-R) to understand how models behave under distribution shifts. In many cases, particular shortcomings can only be explored using synthetic datasets (Cimpoi et al., 2013). Hendrycks & Dietterich (2018) introduced IMAGENET-C, a synthetic set of common corruptions. Geirhos et al. (2018) propose to use images with a texture-shape cue conflict to evaluate the propensity of models to over-emphasize texture cues. Xiao et al. (2020); Sagawa et al. (2020) investigate whether models are biased towards background cues by compositing foreground objects with various background images (IMAGENET-9, WATERBIRDS). In all cases, building such datasets is time-consuming and requires expert knowledge.

Automated failure discovery. In some instances, it is possible to distill rules or specifications that constrain the input space enough to enable the automated discovery of failures via optimization or brute-force search. In vision tasks, adversarial examples, which are constructed using ℓ_p-norm bounded perturbations of the input, can cause neural networks to make incorrect predictions with high confidence (Carlini & Wagner, 2017a;b; Goodfellow et al., 2014; Kurakin et al., 2016; Szegedy et al., 2013). In language tasks, some efforts manually compose templates to generate test cases for specific failures (Jia & Liang, 2017; Garg et al., 2019; Ribeiro et al., 2020). Such approaches rely on human creativity and are intrinsically difficult to scale. Several works (Baluja & Fischer, 2017; Song et al., 2018; Xiao et al., 2018; Qiu et al., 2019; Wong & Kolter, 2021; Laidlaw et al., 2020; Gowal et al., 2019) go beyond hard-coded rules by leveraging generative and perceptual models. However, such approaches are difficult to automate as it is unclear how to relate specific latent variables to isolated structures of the original input. Finally, we highlight a concurrent work (Ge et al., 2022), which leverages captioning and text-to-image models to construct background images to evaluate (and improve) an object detector. Their approach requires compositing the resulting images with foreground objects and is not open-ended, in the sense that it requires a dataset of background images. Perhaps, the work by Perez et al. (2022) on *red-teaming* language models is the most similar to ours.

Perez et al. demonstrate how to prompt a language model to automatically generate test cases to probe another language model for toxic and other unintended output.

Interpretability. Interpretability techniques aim to explain a rationale behind individual model predictions. They surface information that allows a user to inspect how a model behaves. Casper et al. (2022) demonstrate that feature-level attacks, which create adversarial patches, can help diagnose brittle feature associations. However, much like LIME (Ribeiro et al., 2016) or GRAD-CAM (Selvaraju et al., 2019), the results are difficult to understand. Other works (Abid et al., 2022; Jain et al., 2022a; Eyuboglu et al., 2022) leverage auxiliary information in the form of attributes or image-to-text embeddings (e.g., from CLIP; Radford et al., 2021) to provide explanations in natural language. However, these methods often rely on an additional dataset which limits their scope.

3 METHOD

Notation. We consider a classifier $f : \mathbb{X} \rightarrow \mathbb{Y}$, where $\mathbb{X}$ is the set of inputs (i.e., images) and $\mathbb{Y}$ is the label set. We also assume that inputs $\boldsymbol{x} \in \mathbb{X}$ with label $y \in \mathbb{Y}$ are drawn from an underlying distribution $p(\mathbf{x}|\boldsymbol{z}, y)$ conditioned on latent representations $\boldsymbol{z} \in \mathbb{Z}$. In the context of this specific work, $\boldsymbol{z}$ is a textual description of the image $\boldsymbol{x}$. We are interested in discovering captions $\boldsymbol{z}$ corresponding to images $\boldsymbol{x} \sim p(\mathbf{x}|\boldsymbol{z}, y)$ with label y that lead to significantly higher misclassification rates than generic images drawn from the marginal distribution $p(\mathbf{x}|y)$ conditioned solely on the label. Formally, given a label y, we would like to find $\boldsymbol{z}$ with

$$\mathop{\mathbb{E}}_{\boldsymbol{x} \sim p(\mathbf{x}|\boldsymbol{z}, y)} [f(\boldsymbol{x}) \neq y] > \mathop{\mathbb{E}}_{\boldsymbol{x} \sim p(\mathbf{x}|y)} [f(\boldsymbol{x}) \neq y] \tag{1}$$

where $[\cdot]$ represents the Iverson bracket. We may also be interested in identifying specific misclassifications towards a wrong (target) label $\bar{y} \neq y$, and would like that

$$\mathop{\mathbb{E}}_{\boldsymbol{x} \sim p(\mathbf{x}|\boldsymbol{z}, y)} [f(\boldsymbol{x}) = \bar{y}] > \mathop{\mathbb{E}}_{\boldsymbol{x} \sim p(\mathbf{x}|y)} [f(\boldsymbol{x}) = \bar{y}] \,. \tag{2}$$

As we do not have access to the true underlying distributions $p(\mathbf{x}|\boldsymbol{z}, y)$ and $p(\mathbf{x}|y)$, we leverage a large-scale text-to-image model (such as DALL·E 2 or IMAGEN) to approximate them. Similarly, we approximate $p(\mathbf{z}|\boldsymbol{x}, y)$ with a captioning model (e.g., FLAMINGO or LEMON). We denote approximations of these distributions with the symbol $\hat{p}$.

> For each of the following steps, we highlight additional implementation details and explain how we construct prompts for the text-to-image and image-to-text models. Some minute details are omitted as to not break anonymity and will be added later.

Generating failure cases. Our approach is described in Fig. 1. It consists of initially finding *baseline* failures for the underlying model f by sampling inputs $\boldsymbol{x}$ from $\hat{p}(\mathbf{x}|y)$.[1] Given a label of interest y, the output of this step is a set $\mathbb{D} = \{\boldsymbol{x}_i \sim \hat{p}(\mathbf{x}|y)\}_{i=1}^{N}$ (where N is the number of images we wish to generate), a set $\mathbb{D}_{\text{fail}} = \{\boldsymbol{x} \in \mathbb{D} | f(\boldsymbol{x}) \neq y\}$ and an estimate of the baseline failure rate $|\mathbb{D}_{\text{fail}}|/N$ (corresponding to the right-hand side of Eq. 1). In this work, we consider problematic misclassifications only so we restrict ourselves to failures where any of the top-3 predicted labels are not under the same parent as the true label y in the WORDNET hierarchy (Miller, 1995).[2]

> This step leverages a text-to-image generative model conditioned on y with prompts such as *"a realistic photograph of a fly (insect)."*, which are automatically generated from the corresponding class and WORDNET hierarchy. As our domain of interest is composed of real images (much like the images in IMAGENET), the prompt is designed to enforce the generation of photographs of real objects and animals rather than drawings or paintings. Further prompt engineering can be explored to find failures on a wide variety of domains (such as sketches or medical imaging; Hendrycks et al., 2020; Kather et al., 2022).

[1] In practice, it is possible to steer the generation process to induce more frequent failures (e.g., by optimizing latents or conditioning via gradient ascent on the cross-entropy loss; Wong & Kolter, 2021). However, as a proof-of-concept, we assume only black-box access to off-the-shelf text-to-image model.

[2] Other options include considering only misclassifications where the true label is not in the top-k predicted labels or where the confidence in the true label is lower than a predefined threshold.

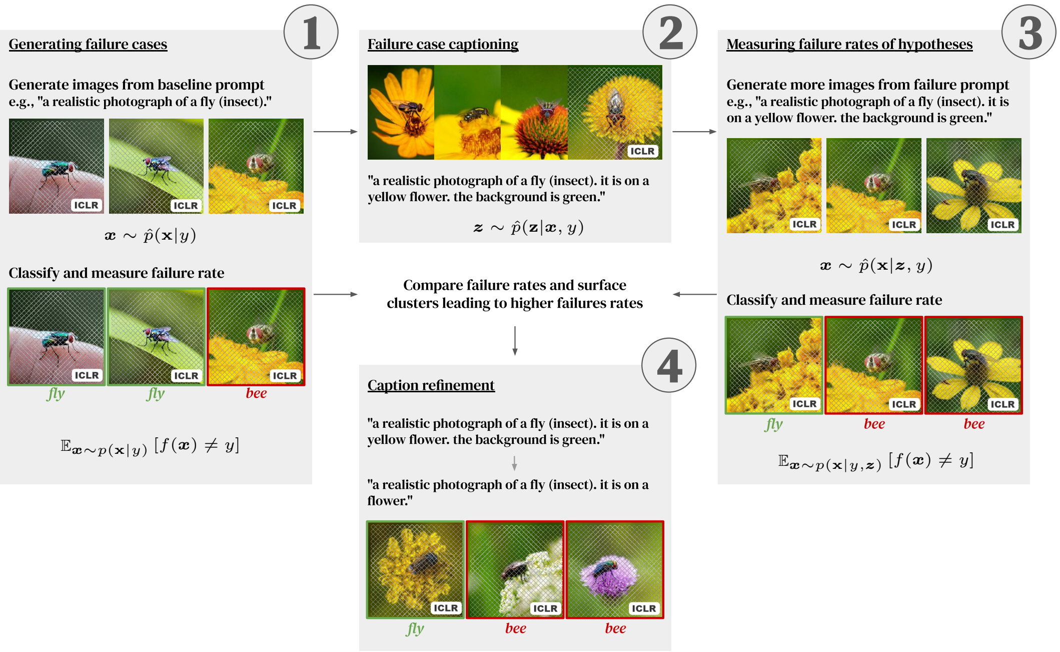
1
Generating failure cases
Generate images from baseline prompt
e.g., "a realistic photograph of a fly (insect)."
ICLR
$\boldsymbol{x} \sim \hat{p}(\mathbf{x}|y)$
Classify and measure failure rate
fly
fly
bee
$\mathbb{E}_{\boldsymbol{x}\sim p(\mathbf{x}|y)}\left[f(\boldsymbol{x}) \neq y\right]$
2
Failure case captioning
"a realistic photograph of a fly (insect). it is on a yellow flower. the background is green."
$\boldsymbol{z} \sim \hat{p}(\mathbf{z}|\boldsymbol{x}, y)$
3
Measuring failure rates of hypotheses
Generate more images from failure prompt
e.g., "a realistic photograph of a fly (insect). it is on a yellow flower. the background is green."
$\boldsymbol{x} \sim \hat{p}(\mathbf{x}|\boldsymbol{z}, y)$
Classify and measure failure rate
fly
bee
bee
$\mathbb{E}_{\boldsymbol{x}\sim p(\mathbf{x}|y,\boldsymbol{z})}\left[f(\boldsymbol{x}) \neq y\right]$
Compare failure rates and surface clusters leading to higher failures rates
4
Caption refinement
"a realistic photograph of a fly (insect). it is on a yellow flower. the background is green."
"a realistic photograph of a fly (insect). it is on a flower."
fly
bee
bee

Figure 1: Diagram of our method. The method starts by generating images containing a given class y to measure the baseline failure rate of that class (right-hand side of Eq. 1). We construct a textual description for each misclassified image. This description is used to produce new images and measure the failure rate on images corresponding to that description (left-hand side of Eq. 1). The final description can be edited (manually or automatically) to understand the source of the failures.

Optional clustering failure cases. Clustering is not necessary, but makes the search for the caption $\boldsymbol{z}$ leading to high failure rates more efficient and computationally manageable. First, we split $\mathbb{D}_{\text{fail}}$ by predicted label, i.e. $\mathbb{D}_{\text{fail}} = \mathbb{D}_{\text{fail}}^{(1)} \cup \ldots \cup \mathbb{D}_{\text{fail}}^{(|\mathcal{Y}|)}$, where $\mathbb{D}_{\text{fail}}^{(y)} = \{\boldsymbol{x} \in \mathbb{D}_{\text{fail}} | f(\boldsymbol{x}) = y\}$. Then, for each subset $\mathbb{D}_{\text{fail}}^{(y)}$, we group inputs that have similar feature representations together (e.g., using the cosine distance between intermediate activations of a pretrained model). Many other choices of clustering method exist. The goal of this step is to reduce the number of clusters to a minimum without amalgamating different causes of failure together.[3]

Failure case captioning. For each cluster $\mathbb{A} \subseteq \mathbb{D}_{\text{fail}}$, we would like to find a caption $\boldsymbol{z}_{\mathbb{A}}$ that describes it. Grounding failures in simple textual descriptions allows us to maintain the diversity of the generated images: the generated images resemble the images leading to the original failure without being exact copies. Ideally, we would like to find the caption $\boldsymbol{z}_{\mathbb{A}}$ that maximizes the likelihood of sampling elements of $\mathbb{A}$, i.e., $\boldsymbol{z}_{\mathbb{A}} = \arg\max_{\boldsymbol{z}} \prod_{\boldsymbol{x}\in\mathbb{A}} \hat{P}(\boldsymbol{x}|\boldsymbol{z}, y)$. We may wish to impose constraints on $\boldsymbol{z}_{\mathbb{A}}$, such as a maximum number of words or sentences.[4] Finding such a caption is computationally hard and measuring exact likelihoods $\hat{P}(\boldsymbol{x}|\boldsymbol{z}, y)$ can be challenging. Hence, we resort to sampling captions directly from a captioning model $\hat{p}(\mathbf{z}|\boldsymbol{x}, y)$ for each image of cluster $\mathbb{A}$.[5] Captions are split into sentences, resulting in a set of sentences $\mathbb{S}$. Sentences are greedily combined (up to a maximum number of sentences K) to maximize the likelihood of sampling the overall caption $\boldsymbol{z}_{\mathbb{A}} = [\boldsymbol{s}_1, \ldots, \boldsymbol{s}_K]$ with $\boldsymbol{s}_j = \arg\max_{\boldsymbol{s}\in\mathbb{S}} \prod_{\boldsymbol{x}\in\mathbb{A}} \hat{P}([\boldsymbol{s}_1, \ldots, \boldsymbol{s}_{j-1}, \boldsymbol{s}]|\boldsymbol{x}, y)$ and $\boldsymbol{s}_1 = \arg\max_{\boldsymbol{s}\in\mathbb{S}} \prod_{\boldsymbol{x}\in\mathbb{A}} \hat{P}([\boldsymbol{s}]|\boldsymbol{x}, y)$. If no clustering is performed, we can directly sample a caption $\boldsymbol{z}_{\{\boldsymbol{x}\}} \sim \hat{p}(\mathbf{z}|\boldsymbol{x}, y)$ from the captioning model for each element $\boldsymbol{x}$ in $\mathbb{D}_{\text{fail}}$. Each caption serves as a failure hypothesis.

[3] Wrongful clustering may lead the next step to produce descriptions that fail to induce more failures. As a result, we may miss failures that we would have discovered without clustering, but the failures that we do discover remain valid.

[4] These constraints guarantee that captions remain simple and not overly descriptive.

[5] This formulation implicitly assumes that any caption is as likely as another under a given label y, which in general does not hold true, but serves as a reasonable approximation.

> This step leverages an image-to-text captioning model and forces descriptive completions via few-shot prompting. In particular, we use three shots, with each shot being an image and caption pair. Images are publicly available online and are manually described using between four to seven short sentences that describe the subject of the photograph and its physical position with respect to the camera, as well as the background or context in which the subject appears (see Appendix A for more details). To condition on y, we force the captioning model to only consider completions to the original baseline prompt, which guarantees that the final caption contains the true label. An example of a resulting caption is *"a realistic photograph of a fly (insect). the background is blurred. the fly is in focus. it is on a yellow flower. the background is green."* Each caption serves as a failure hypothesis.

Measuring failure rates of hypotheses. For each failure hypothesis or caption $\boldsymbol{z}_{\mathbb{A}}$, we can measure its failure rate via sampling $\mathbb{E}_{\boldsymbol{x}\sim p(\mathbf{x}|\boldsymbol{z}_{\mathbb{A}},y)}\left[f(\boldsymbol{x}) \neq y\right]$.This step allows us to surface captions $\boldsymbol{z}^{\star}$ that satisfy Eq. 1 (or alternatively Eq. 2) by comparing the resulting failure rate with the baseline failure rate obtained initially.

> Much like the first step on generating the baseline failure cases, this step uses the text-to-image model, which we now prompt with descriptive cluster captions such as *"a realistic photograph of a fly (insect). the background is blurred. the fly is in focus. it is on a yellow flower. the background is green."*

Caption refinement and counterfactual analysis. Given a caption $\boldsymbol{z}^{\star}$, we would like to provide a shorter, self-contained caption that obtains a similar failure rate. For this step, we rely on simple rules[6] and evaluate promising caption rewrites. Finally, as captions are human-readable, users can interact with the system and test alternative hypotheses.

> In our implementation, we exploit two rules: *(i)* we evaluate all individual sentences (for our ongoing example, these would be *"the background is blurred"*, *"the fly is in focus"*, *"it is on a yellow flower"* and *"the background is green"*) in conjunction with the original prompt (e.g., *"a realistic photograph of a fly (insect)"*); *(ii)* the most promising prompt is further refined by dropping adjectives (such as *"yellow"* in *"it is on a yellow flower"*). More sophisticated rules and rewrites are possible (Ribeiro et al., 2018). Alternatively, we could leverage a large-language model via few-shot prompting to automate this process (Witteveen & Andrews, 2019).

Finally, we note that it is possible to use part of this pipeline to understand known failure cases (e.g., on failures reported by external users of the model f).

4 Results

In this section, we elaborate on two use-cases. In the first, we find failure cases of a Residual Network (ResNet) (He et al., 2016) model with 50 layers (ResNet-50), trained on ImageNet, in an open-ended manner. We focus on three arbitrarily chosen labels and show that the failures we obtain arise from consistent misclassifications caused by spurious correlations. In the second use-case, we show that we can generate failures at scale for various models. We leverage ImageNet-A as a source of initial failures and create new variants of ImageNet-A that target specific model architectures.

4.1 Open-ended failure search

Setup. We evaluate a ResNet-50 trained on ImageNet and available on Tf-Hub.[7] We select three labels y at random: `Persian cat`, `fly` and `crayfish`. For each label y, we manually select target labels $\bar{y}$ (`snow leopard`, `bee` and `chainlink fence` respectively) and execute the protocol defined in Sec. 3. At each step, we sample images from the generative model until we gather 20 images that are misclassified as the target label $\bar{y}$ and compute failure rates at that point. Fig. 2 and Table 1 show these automatically discovered failures. More failures for additional true and

[6] This may seem at odds with our claim on open-endedness. However, we note that this step is optional and its goal is simply to produce shorter failure descriptions.

[7] https://tfhub.dev/google/imagenet/resnet_v2_50/classification/5

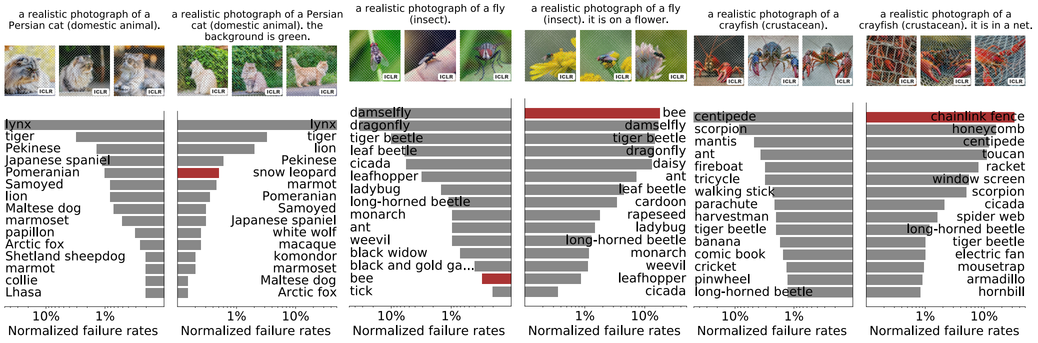

(a) Persian cat → Snow leopard (b) Fly → Bee (c) Crayfish → Chainlink fence

Figure 2: Distribution of failures of a ResNet-50 for the baseline and automatically discovered captions for three true and target label pairs. For each panel, failures resulting from the baseline caption are on the left and failures resulting from the discovered caption are on the right. We show the top-15 mistakes and three randomly sampled images for each caption. We highlight in red the bar corresponding to the target label. Absolute failure rates are given in Table 1.

True label	Target label	Caption	Failure rate (any)		Failure rate (target)	
Persian cat	Snow leopard	a realistic photograph of a Persian cat (domestic animal).	0.11%	1×	0.00022%	1×
		— " — the background is green.	0.64%	6×	0.0032%	14×
Fly	Bee	a realistic photograph of a fly (insect).	0.48%	1×	0.0014%	1×
		— " — it is on a flower.	4.11%	9×	0.72%	497×
Crayfish	Chainlink fence	a realistic photograph of a crayfish (crustacean).	0.93%	1×	0.00047%	1×
		— " — it is in a net.	6.31%	7×	1.73%	3721×

Table 1: Absolute failure rates of a ResNet-50 for three true and target label pairs. We show the total failure rate (i.e., the model prediction is different from the true label) and the target failure rate (i.e., the model prediction is the target label). Captions are automatically discovered using the method detailed in Sec. 3.[8]

target label pairs are in Sec. B.1 in the appendix. In Sec. B.1, we also evaluate other architectures (i.e., ViTs) and demonstrate that the discovered captions yield failure rates that are statistically significant.

Discovered failures. Fig. 2(a) shows the distribution of failures for the baseline label Persian cat. We observe that the most frequent confusion, on images generated using the baseline caption *"a realistic photograph of a Persian cat (domestic animal)."* is with lynx. This mistake arises about 0.1% of the time and constitutes 87.3% of all failures. In comparison, the confusion with snow leopard is rather infrequent and arises only 0.00022% of the time. Our approach automatically discovers that adding *"the background is green."* to the caption results in a large increase in failure rates. Failures are 5.72× more likely and the model is 14.3× more likely to predict snow leopard. We generally observe that mistakes with wild animals become more prevalent when the cat is outdoors. Similarly, Fig. 2(b) and Fig. 2(c) show failures on images of flies and crayfish, respectively. Flies on flowers are significantly more likely to be confused for bees when they are on flowers (497×), while crayfish in nets are more frequently confused as chainlink fences (3721×), honeycomb, window screens or spider webs. These highlight two shortcomings of the underlying classifier: *(i)* the over-reliance on spurious cues (such as the flower); *(ii)* the inability to determine which object is the main subject of a photograph (e.g., which of the net or crayfish is important).

Generalizability of failure descriptions. To verify that the discovered failures are not specific to the text-to-image model used in this manuscript and do not result from artifacts in the image generation process, we generate 30 images using the baseline and discovered captions with Dall·E 2 and Stable-Diffusion (samples are shown in Fig. 13 and Fig. 14 in the appendix). We evaluate

[8] As a point of comparison, we can also evaluate the baseline failure rates on images from the ImageNet test set. For Persian cat, fly and crayfish the baseline failure rates are 16%, 8% and 18%, respectively (the target failure rate is 0% for all labels). These failure rates are higher than on images generated by the generative model, this is perhaps indicating that the generative model produces images that are more canonical and conservative. We also point out that we generate 9.1M samples to compute the first row of the table, 625K for the second and 1.4M, 2.8K, 4.3M, 1.2K for the subsequent rows.

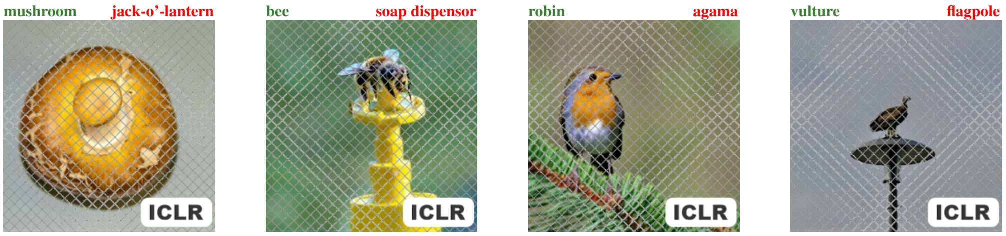

Figure 3: Examples of failures automatically found in In-G-Rn. The correct label is to the left in **green**. The incorrect prediction is to the right in **red**. Images are not watermarked upon classification.

the failure rates for the `fly` and `crayfish` labels (which exhibited higher failure rates). With Dall·e 2, for the 30 images generated with the prompt *"a realistic photograph of a fly (insect)."*, 18 are correctly classified as flies and none are classified as bees. When adding *"it is on a flower."* to the prompt, the overall failure rate increases (only 14 images are correctly classified) and nine images are now classified as bees. Similarly, for *"a realistic photograph of a crayfish (crustacean)."*, 29 images are correctly classified as either `crayfish`, `spiny lobster`, `American lobster`, `Dungeness crab` or `king crab`, while none are classified as `chainlink fence`. When adding *"it is in a net."*, four are classified as `chainlink fence` (with `chainlink fence` appearing ten times in the top-3 predictions), while only 21 images are correctly classified. Results are similar for Stable-Diffusion images.[9] Overall, we observe that discovered failures generalize across generative models. Finally, we also leverage *Google Image Search*[10] to find 30 images for each of the following queries: *"fly"*, *"fly on flower"*, *"crayfish"*, *"crayfish in net"* (images must have a resolution of at least 256×256 and should contain the true label). We classify all images and observe that the number of failures towards `bee` increases from zero to two and those towards `chainlink fence` increase from zero to four. This illustrates again that discovered failures are general and extend to real photographs.

4.2 Adversarial dataset generation at scale

We demonstrate how to apply our automated pipeline to generate large datasets of failures. We seed our search by captioning images from ImageNet-A. We show that the discovered failures generalize across initializations of a given model architecture and between models of different architectures.

Generating large-scale datasets. We assume that we have access to a set of captions that describe potential failure cases.[11] These captions are automatically extracted from the 7,500 images of ImageNet-A using the captioning model, limiting its output to two sentences maximum. For each caption, we sample up to a thousand images keeping those leading to misclassifications and limit the number of misclassified images kept per caption. We consider two models: a ResNet-50 (abbreviated hereafter by Rn) and a Vision Transformer in its B/16 variant (Dosovitskiy et al., 2020), abbreviated by ViT. Both models are trained solely on ImageNet and achieve 76% and 80% top-1 accuracy, respectively. This yields two separate datasets of failures which we refer to as In-G-Rn and In-G-ViT that are of size 12,332 and 9,536 respectively.

Visualizations of failure cases. Samples from In-G-Rn are shown in Fig. 3, with true and predicted labels. We can see that while the images clearly show the correct class, the model erroneously predicts a different one. Additional samples for both In-G-Rn and In-G-ViT are visible in Fig. 15 and Fig. 16 (in the appendix). Appendix C provides an analysis for some failure cases found in In-G-ViT and details how images from the ImageNet training set may have misled the classifier.

Generalizability of failure cases. To investigate whether the discovered failures generalize across initializations, we train an additional ResNet (Rn2) and ViT (ViT2) on ImageNet with the exact

[9] For Stable-Diffusion, the number of failures increases from one to two and from four to 16, for the `fly` and `crayfish` labels, respectively.

[10] https://images.google.com

[11] This assumption is not necessary. However, it accelerates our search by generating images that are more likely to induce failures.

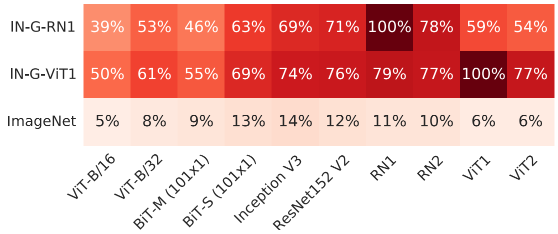

Figure 4: Failure rates (top-3) for different models on two generated datasets and IMAGENET. We report the failure rates of different models trained on IMAGENET.

Dataset	FID ↓	KID ↓
IMAGENET-A	56.6	0.0460
IN-G-RN	48.3	0.0305
IN-G-VIT	53.9	0.0330
IMAGENET (train)	2.3	0.0003

Table 2: FID and KID scores. We report FID and KID scores in relation to IMAGENET (test).

same setup as our two original models but different random seeds. We also consider a large set of additional models trained on IMAGENET and optionally pre-trained on larger datasets obtained from TF-HUB. Fig. 4 shows the failure rates induced by both datasets on all models (failures are accounted when the top-3 predictions do not include the true label). First, we observe that failures transfer well between models of the same architecture. Indeed, 78% of the failures in IN-G-RN transfer to RN2, while the ones in IN-G-VIT transfer with 77% chance to VIT2. Second, we observe that failures for a given model architecture transfer to a large extent across architectures. Even when large-scale pretraining is used (with the BIT-M (101x1), VIT-B/16 and VIT-B/32 models pretrained on IMAGENET21K), failures transfer at a rate of 39-53% for IN-G-RN and 50-61% for IN-G-VIT. Further results for additional models are in Sec. B.2 in the appendix.

Distribution shift. Finally, we compare our generated datasets to IMAGENET and IMAGENET-A. The aim is to validate that we generate images that are similar to those in IMAGENET. We compute the Fréchet Inception Distance (FID; Heusel et al., 2017) and the Kernel Inception Distance (KID; Binkowski et al., 2018) between the generated images and the IMAGENET test set. Table 2 also shows the FID and KID of the IMAGENET train set and IMAGENET-A. We find that our generated images are *more* similar to those from IMAGENET under both metrics than those from IMAGENET-A.

5 DISCUSSION AND LIMITATIONS

The motivation behind our work is to develop a proof-of-concept demonstrating that today's large-scale text-to-image and image-to-text models can be leveraged to find human-interpretable failures in vision models. While we focus exclusively on IMAGENET, there are encouraging signs that these generative models could be used to probe models trained on specialized tasks such as medical imaging (Kather et al., 2022). Overall, there remain a number of key challenges to address.

Coverage. While our approach can successfully be used to demonstrate the presence of failures, it is important to understand that (just like scraping the web) it cannot prove their absence. In other words, there is no guarantee that it will discover all failures of a given model.[12] Moreover, the generative model is only an approximation of the distribution of interest and may lack coverage. For example, it might almost never generate "a lawnmower falling down from the sky" (an actual image from the IMAGENET training set; Jain et al., 2022b) when prompted with *"a realistic photograph of a lawnmower"*. While this can help ground failures to scenes that are likely to occur in the real-world, it also means that rare failures are unlikely to be discovered (see Fig. 5(a)).

Bias. While we take the view here that off-the-shelf large-scale generative models are trained on diverse and unbiased data, the reality is far from it: these models mirror the distribution of images and captions seen on the web. The generative model may over-sample particular regions of the image manifold and, as a result, our approach is more likely to discover failures in these high-density regions and miss failures pertaining to other regions (see Fig. 5(b)). Possible solutions to reduce bias include clever prompting (which introduces expert knowledge) or discovering failure prompts more actively by avoiding random sampling (e.g., through adversarial techniques).

[12] However, if the generative model matches the true distribution of images, it is possible to provide meaningful probabilistic guarantees.

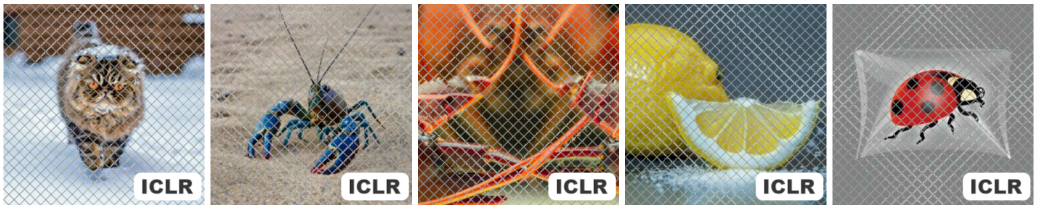

(a) Coverage (b) Bias (c) Captioning issues (d) Generation issues (e) OOD sampling

Figure 5: Illustrative examples of various challenges. (a) Persian cats in snow (generated using *“a realistic photograph of a Persian cat (domestic animal). it is walking in the snow.”*) are misclassified as snow leopards at a rate of 0.016%, which is significantly higher than the failure rate of 0.0032% induced by the automatically found caption (*“— ” — the background is green.”*); the total failure rate also increases twelve-fold to 8.15% (from 0.64%). (b) It is estimated that only 1 in 10,000 crayfish turn blue. However, 9% of the images generated using *“a realistic photograph of a crayfish (crustacean).”* contain a blue crayfish (estimated by manually looking at 100 samples). (c) This image of a crayfish is misclassified as a chainlink fence. The output of the captioning model for this particular image is *“a realistic photograph of a crayfish. the crayfish is very detailed. the crayfish is facing the camera. the crayfish is orange. it has two antennae.”* While the caption describes the image, it does not provide enough detail to reconstruct the image. (d) This image is generated from the caption *“a realistic photograph of a saltshaker (container). there is a lemon slice on the side of the salt shaker.”* While the image contains a lemon, the true class y (`saltshaker`) is not visible. (e) Generated with the caption *“a realistic photograph of a ladybug (insect). it is in a plastic bag.”*, this image illustrates that text-to-image models can create image that are not from the intended distribution (i.e., of realistic photographs).

Captioning issues. Using captions as our latent representation allows our approach to produce human-interpretable explanations and constrains our search to failures that can be explained in words. Not only is it possible for the captioning model to miss important details or produce ungrounded captions, but some failures may simply be hard to describe (even by a human). As a result, newly generated images may look different from the set of images that induced the original failure. We note that efficiently enforcing consistency between the generated and original images (through a common caption) is an open problem since we would like to search over *reasonable* captions that are likely to produce images corresponding to the original failure. Fig. 5(c) shows an example. The figure shows a `crayfish` misclassified as a `chainlink fence`. While the reason for that failure is immediately obvious to us, it remains difficult to describe with a succinct caption.

Image generation issues. While the text-to-image model may make occasional mistakes (such as generating the wrong object for unambiguous prompts), subtle errors can also arise from the interplay between the model and its prompt. The prompt may be ambiguous, such as using words that have multiple meanings (e.g., a *“walking stick”* can be both a cane or an insect), or may describe multiple objects with complex relationships that exacerbate mistakes (see Fig. 5(d)).

Out-of-distribution sampling. Ensuring that images sampled from an off-the-shelf generative model are part of the intended distribution (e.g., resembling IMAGENET) is difficult. We start our prompts with *“a realistic photograph”* in a bid to help steer the approximated distribution $\hat{p}(\mathbf{x}|y, \boldsymbol{z})$ away from artistic drawings and closer to the true distribution $p(\mathbf{x}|y, \boldsymbol{z})$. This approach is effective, but not always successful (see Fig. 5(e)). In some cases, finding a suitable prompt is not obvious (e.g., to output images from a particular medical domain; Kather et al., 2022) and fine-tuning models on the dataset of interest may be necessary.

Privacy. As we are generating large amounts of data, it is important to consider the associated privacy risks. While these risks can be mitigated by using generative models trained on public, non-sensitive data, more research on private generative modelling is necessary (Harder et al., 2022).

Despite these challenges, we foresee that large-scale generative models will increasingly be used as debugging tools. In this work, we introduced an automated pipeline that discovers failure cases in vision models. It constitutes a proof-of-concept that such a system allows for large-scale investigations of vision models in an open-ended manner.

REFERENCES

Abubakar Abid, Mert Yuksekgonul, and James Zou. Meaningfully debugging model mistakes using conceptual counterfactual explanations. In *International Conference on Machine Learning*. PMLR, 2022. 3

Jean-Baptiste Alayrac, Jeff Donahue, Pauline Luc, Antoine Miech, Iain Barr, Yana Hasson, Karel Lenc, Arthur Mensch, Katie Millican, Malcolm Reynolds, Roman Ring, Eliza Rutherford, Serkan Cabi, Tengda Han, Zhitao Gong, Sina Samangooei, Marianne Monteiro, Jacob Menick, Sebastian Borgeaud, Andrew Brock, Aida Nematzadeh, Sahand Sharifzadeh, Mikolaj Binkowski, Ricardo Barreira, Oriol Vinyals, Andrew Zisserman, and Karen Simonyan. Flamingo: a visual language model for few-shot learning. *arXiv preprint arXiv:2204.14198*, 2022. 1

Martin Arjovsky, Léon Bottou, Ishaan Gulrajani, and David Lopez-Paz. Invariant risk minimization. *arXiv preprint arXiv:1907.02893*, 2019. 1

Shumeet Baluja and Ian Fischer. Adversarial transformation networks: Learning to generate adversarial examples. *arXiv preprint arXiv:1703.09387*, 2017. 2

Battista Biggio, Igino Corona, Davide Maiorca, Blaine Nelson, Nedim Srndic, Pavel Laskov, Giorgio Giacinto, and Fabio Roli. Evasion Attacks against Machine Learning at Test Time. *arXiv preprint arXiv:1708.06131*, 2013. 25

Mikolaj Binkowski, Dougal J. Sutherland, Michael Arbel, and Arthur Gretton. Demystifying MMD GANs. In *International Conference on Learning Representations*, 2018. 8

Mariusz Bojarski, Davide Del Testa, Daniel Dworakowski, Bernhard Firner, Beat Flepp, Prasoon Goyal, Lawrence D. Jackel, Mathew Monfort, Urs Muller, Jiakai Zhang, Xin Zhang, Jake Zhao, and Karol Zieba. End to end learning for self-driving cars. *arXiv preprint arXiv:1604.07316*, 2016. 1

Rishi Bommasani, Drew A. Hudson, Ehsan Adeli, Russ Altman, Simran Arora, Sydney von Arx, Michael S. Bernstein, Jeannette Bohg, Antoine Bosselut, Emma Brunskill, Erik Brynjolfsson, Shyamal Buch, Dallas Card, Rodrigo Castellon, Niladri Chatterji, Annie Chen, Kathleen Creel, Jared Quincy Davis, Dora Demszky, Chris Donahue, Moussa Doumbouya, Esin Durmus, Stefano Ermon, John Etchemendy, Kawin Ethayarajh, Li Fei-Fei, Chelsea Finn, Trevor Gale, Lauren Gillespie, Karan Goel, Noah Goodman, Shelby Grossman, Neel Guha, Tatsunori Hashimoto, Peter Henderson, John Hewitt, Daniel E. Ho, Jenny Hong, Kyle Hsu, Jing Huang, Thomas Icard, Saahil Jain, Dan Jurafsky, Pratyusha Kalluri, Siddharth Karamcheti, Geoff Keeling, Fereshte Khani, Omar Khattab, Pang Wei Koh, Mark Krass, Ranjay Krishna, Rohith Kuditipudi, Ananya Kumar, Faisal Ladhak, Mina Lee, Tony Lee, Jure Leskovec, Isabelle Levent, Xiang Lisa Li, Xuechen Li, Tengyu Ma, Ali Malik, Christopher D. Manning, Suvir Mirchandani, Eric Mitchell, Zanele Munyikwa, Suraj Nair, Avanika Narayan, Deepak Narayanan, Ben Newman, Allen Nie, Juan Carlos Niebles, Hamed Nilforoshan, Julian Nyarko, Giray Ogut, Laurel Orr, Isabel Papadimitriou, Joon Sung Park, Chris Piech, Eva Portelance, Christopher Potts, Aditi Raghunathan, Rob Reich, Hongyu Ren, Frieda Rong, Yusuf Roohani, Camilo Ruiz, Jack Ryan, Christopher Ré, Dorsa Sadigh, Shiori Sagawa, Keshav Santhanam, Andy Shih, Krishnan Srinivasan, Alex Tamkin, Rohan Taori, Armin W. Thomas, Florian Tramèr, Rose E. Wang, William Wang, Bohan Wu, Jiajun Wu, Yuhuai Wu, Sang Michael Xie, Michihiro Yasunaga, Jiaxuan You, Matei Zaharia, Michael Zhang, Tianyi Zhang, Xikun Zhang, Yuhui Zhang, Lucia Zheng, Kaitlyn Zhou, and Percy Liang. On the opportunities and risks of foundation models. *arXiv preprint arXiv:2108.07258*, 2021. 2

Joy Buolamwini and Timnit Gebru. Gender shades: Intersectional accuracy disparities in commercial gender classification. In *Conference on Fairness, Accountability and Transparency*, 2018. 1

Nicholas Carlini and David Wagner. Adversarial examples are not easily detected: Bypassing ten detection methods. In *Proceedings of the ACM Workshop on Artificial Intelligence and Security*, 2017a. 2

Nicholas Carlini and David Wagner. Towards evaluating the robustness of neural networks. In *2017 IEEE Symposium on Security and Privacy*, 2017b. 2

Stephen Casper, Max Nadeau, Dylan Hadfield-Menell, and Gabriel Kreiman. Robust feature-level adversaries are interpretability tools. *arXiv preprint arXiv:2110.03605*, 2022. 3

Myung Jin Choi, Antonio Torralba, and Alan S Willsky. Context models and out-of-context objects. *Pattern Recognition Letters*, 2012. 2

Mircea Cimpoi, Subhransu Maji, Iasonas Kokkinos, Sammy Mohamed, and Andrea Vedaldi. Describing textures in the wild. *arXiv preprint arXiv:1311.3618*, 2013. 2

Jeffrey De Fauw, Joseph R Ledsam, Bernardino Romera-Paredes, Stanislav Nikolov, Nenad Tomasev, Sam Blackwell, Harry Askham, Xavier Glorot, Brendan O'Donoghue, Daniel Visentin, George van den Driessche, Balaji Lakshminarayanan, Clemens Meyer, Faith Mackinder, Simon Bouton, Kareem Ayoub, Reena Chopra, Dominic King, Alan Karthikesalingam, Cían O Hughes, Rosalind Raine, Julian Hughes, Dawn A Sim, Catherine Egan, Adnan Tufail, Hugh Montgomery, Demis Hassabis, Geraint Rees, Trevor Back, Peng T Khaw, Mustafa Suleyman, Julien Cornebise, Pearse A Keane, and Olaf Ronneberger. Clinically applicable deep learning for diagnosis and referral in retinal disease. In *Nature Medicine*, 2018. 1

Jia Deng, Wei Dong, Richard Socher, Li-Jia Li, Kai Li, and Li Fei-Fei. Imagenet: A large-scale hierarchical image database. In *Proceedings of the IEEE/CVF Conference on Computer Vision and Pattern Recognition*, 2009. 2

Alexey Dosovitskiy, Lucas Beyer, Alexander Kolesnikov, Dirk Weissenborn, Xiaohua Zhai, Thomas Unterthiner, Mostafa Dehghani, Matthias Minderer, Georg Heigold, Sylvain Gelly, Jakob Uszkoreit, and Neil Houlsby. An Image is Worth 16x16 Words: Transformers for Image Recognition at Scale. *arXiv preprint arXiv:2010.11929*, 2020. 7, 18

Sabri Eyuboglu, Maya Varma, Khaled Saab, Jean-Benoit Delbrouck, Christopher Lee-Messer, Jared Dunnmon, James Zou, and Christopher Ré. Domino: Discovering systematic errors with cross-modal embeddings. *arXiv preprint arXiv:2203.14960*, 2022. 3

Sahaj Garg, Vincent Perot, Nicole Limtiaco, Ankur Taly, Ed H. Chi, and Alex Beutel. Counterfactual fairness in text classification through robustness. In *Proceedings of the AAAI/ACM Conference on AI, Ethics, and Society*, 2019. 2

Yunhao Ge, Jiashu Xu, Brian Nlong Zhao, Laurent Itti, and Vibhav Vineet. Dall-e for detection: Language-driven context image synthesis for object detection. *arXiv preprint arXiv:2206.09592*, 2022. 2

Robert Geirhos, Patricia Rubisch, Claudio Michaelis, Matthias Bethge, Felix A Wichmann, and Wieland Brendel. ImageNet-trained CNNs are biased towards texture; increasing shape bias improves accuracy and robustness. In *International Conference on Learning Representations*, 2018. 2

Robert Geirhos, Jörn-Henrik Jacobsen, Claudio Michaelis, Richard Zemel, Wieland Brendel, Matthias Bethge, and Felix A Wichmann. Shortcut learning in deep neural networks. In *Nature Machine Intelligence*, 2020a. 1, 2

Robert Geirhos, Kristof Meding, and Felix A. Wichmann. Beyond accuracy: quantifying trial-by-trial behaviour of cnns and humans by measuring error consistency. In *Advances in Neural Information Processing Systems*. 2020b. 2

Robert Geirhos, Kantharaju Narayanappa, Benjamin Mitzkus, Tizian Thieringer, Matthias Bethge, Felix A Wichmann, and Wieland Brendel. Partial success in closing the gap between human and machine vision. *Advances in Neural Information Processing Systems*, 2021. 19

Robert Geirhos, Patricia Rubisch, Claudio Michaelis, Matthias Bethge, Felix A Wichmann, and Wieland Brendel. Imagenet-trained cnns are biased towards texture; increasing shape bias improves accuracy and robustness. In *International Conference on Learning Representations*, 2022. 1

Ian Goodfellow, Yoshua Bengio, and Aaron Courville. *Deep Learning*. MIT Press, 2016. 1

Ian J Goodfellow, Jonathon Shlens, and Christian Szegedy. Explaining and harnessing adversarial examples. *arXiv preprint arXiv:1412.6572*, 2014. 2

Sven Gowal, Chongli Qin, Po-Sen Huang, Taylan Cemgil, Krishnamurthy Dvijotham, Timothy Mann, and Pushmeet Kohli. Achieving Robustness in the Wild via Adversarial Mixing with Disentangled Representations. *arXiv preprint arXiv:1912.03192*, 2019. 2

Fredrik Harder, Milad Jalali Asadabadi, Danica J. Sutherland, and Mijung Park. Differentially private data generation needs better features. *arXiv preprint arXiv:2205.12900*, 2022. 9

Kaiming He, Xiangyu Zhang, Shaoqing Ren, and Jian Sun. Deep residual learning for image recognition. *Proceedings of the IEEE Conference on Computer Vision and Pattern Recognition*, 2016. 5, 18

Dan Hendrycks and Thomas Dietterich. Benchmarking Neural Network Robustness to Common Corruptions and Perturbations. In *International Conference on Learning Representations*, 2018. 2

Dan Hendrycks, Kevin Zhao, Steven Basart, Jacob Steinhardt, and Dawn Song. Natural adversarial examples. *arXiv preprint arXiv:1907.07174*, 2019. 1, 2

Dan Hendrycks, Steven Basart, Norman Mu, Saurav Kadavath, Frank Wang, Evan Dorundo, Rahul Desai, Tyler Zhu, Samyak Parajuli, Mike Guo, Dawn Song, Jacob Steinhardt, and Justin Gilmer. The Many Faces of Robustness: A Critical Analysis of Out-of-Distribution Generalization. *arXiv preprint arXiv:2006.16241*, 2020. 1, 2, 3

Martin Heusel, Hubert Ramsauer, Thomas Unterthiner, Bernhard Nessler, and Sepp Hochreiter. Gans trained by a two time-scale update rule converge to a local nash equilibrium. In *Advances in Neural Information Processing Systems*. 2017. 8

Geoffrey Hinton, Li Deng, Dong Yu, George E Dahl, Abdel-rahman Mohamed, Navdeep Jaitly, Andrew Senior, Vincent Vanhoucke, Patrick Nguyen, Tara N Sainath, and others. Deep neural networks for acoustic modeling in speech recognition: The shared views of four research groups. *IEEE Signal processing magazine*, (6), 2012. 1

Xiaowei Hu, Zhe Gan, Jianfeng Wang, Zhengyuan Yang, Zicheng Liu, Yumao Lu, and Lijuan Wang. Scaling up vision-language pre-training for image captioning. *arXiv preprint arXiv:2111.12233*, 2021. 1

Saachi Jain, Hannah Lawrence, Ankur Moitra, and Aleksander Madry. Distilling model failures as directions in latent space. *arXiv preprint arXiv:2206.14754*, 2022a. 3

Saachi Jain, Hadi Salman, Alaa Khaddaj, Eric Wong, Sung Min Park, and Aleksander Madry. A data-based perspective on transfer learning. *arXiv preprint arXiv:2207.05739*, 2022b. 8

Robin Jia and Percy Liang. Adversarial examples for evaluating reading comprehension systems. *arXiv preprint arXiv:1707.07328*, 2017. 2

Jakob Nikolas Kather, Narmin Ghaffari Laleh, Sebastian Foersch, and Daniel Truhn. Medical domain knowledge in domain-agnostic generative ai. In *npj Digital Medicine*, 2022. 3, 8, 9

Aditya Khosla, Tinghui Zhou, Tomasz Malisiewicz, Alexei A Efros, and Antonio Torralba. Undoing the damage of dataset bias. In *European Conference on Computer Vision*, 2012. 2

Alexander Kolesnikov, Lucas Beyer, Xiaohua Zhai, Joan Puigcerver, Jessica Yung, Sylvain Gelly, and Neil Houlsby. Big transfer (bit): General visual representation learning. In *European conference on computer vision*, 2020. 18

Alex Krizhevsky, Ilya Sutskever, and Geoffrey E Hinton. Imagenet classification with deep convolutional neural networks. In *Advances in neural information processing systems*, 2012. 1

Andrey Kuehlkamp, Benedict Becker, and Kevin Bowyer. Gender-from-iris or gender-from-mascara? In *IEEE Winter Conference on Applications of Computer Vision*, 2017. 1

Alexey Kurakin, Ian Goodfellow, and Samy Bengio. Adversarial examples in the physical world. *arXiv preprint arXiv:1607.02533*, 2016. 2

Cassidy Laidlaw, Sahil Singla, and Soheil Feizi. Perceptual Adversarial Robustness: Defense Against Unseen Threat Models. *arXiv preprint arXiv:2006.12655*, 2020. 2

Sebastian Lapuschkin, Stephan Wäldchen, Alexander Binder, Grégoire Montavon, Wojciech Samek, and Klaus-Robert Müller. Unmasking clever hans predictors and assessing what machines really learn. In *Nature Communications*, 2019. 2

Horia Mania, John Miller, Ludwig Schmidt, Moritz Hardt, and Benjamin Recht. Model similarity mitigates test set overuse. In *Advances in Neural Information Processing Systems*. 2019. 2

Henry B Mann and Donald R Whitney. On a test of whether one of two random variables is stochastically larger than the other. *The annals of mathematical statistics*, pp. 50–60, 1947. 18

George A Miller. Wordnet: a lexical database for english. *Communications of the ACM*, 1995. 3

Ethan Perez, Saffron Huang, Francis Song, Trevor Cai, Roman Ring, John Aslanides, Amelia Glaese, Nat McAleese, and Geoffrey Irving. Red teaming language models with language models. *arXiv preprint arXiv:2202.03286*, 2022. 2, 3

Haonan Qiu, Chaowei Xiao, Lei Yang, Xinchen Yan, Honglak Lee, and Bo Li. SemanticAdv: Generating Adversarial Examples via Attribute-conditional Image Editing. *arXiv preprint arXiv:1906.07927*, 2019. 2

Alec Radford, Jong Wook Kim, Chris Hallacy, Aditya Ramesh, Gabriel Goh, Sandhini Agarwal, Girish Sastry, Amanda Askell, Pamela Mishkin, Jack Clark, Gretchen Krueger, and Ilya Sutskever. Learning Transferable Visual Models From Natural Language Supervision. *OpenAI Blog*, 2021. 3

Aditya Ramesh, Prafulla Dhariwal, Alex Nichol, Casey Chu, and Mark Chen. Hierarchical text-conditional image generation with clip latents. *arXiv preprint arXiv:2204.06125*, 2022. 1

Benjamin Recht, Rebecca Roelofs, Ludwig Schmidt, and Vaishaal Shankar. Do ImageNet Classifiers Generalize to ImageNet? *arXiv preprint arXiv:1902.10811*, 2019. 1, 2

Marco Tulio Ribeiro, Sameer Singh, and Carlos Guestrin. ”why should i trust you?”: Explaining the predictions of any classifier. *arXiv preprint arXiv:1602.04938*, 2016. URL `https://arxiv.org/pdf/1602.04938`. 3

Marco Tulio Ribeiro, Sameer Singh, and Carlos Guestrin. Semantically equivalent adversarial rules for debugging NLP models. In *Proceedings of the Annual Meeting of the Association for Computational Linguistics*, 2018. 5

Marco Tulio Ribeiro, Tongshuang Wu, Carlos Guestrin, and Sameer Singh. Beyond accuracy: Behavioral testing of NLP models with CheckList. In *Proceedings of the 58th Annual Meeting of the Association for Computational Linguistics*, 2020. 2

Robin Rombach, Andreas Blattmann, Dominik Lorenz, Patrick Esser, and Björn Ommer. High-resolution image synthesis with latent diffusion models. In *Proceedings of the IEEE/CVF Conference on Computer Vision and Pattern Recognition*, 2022. 1

Shiori Sagawa, Pang Wei Koh, Tatsunori B. Hashimoto, and Percy Liang. Distributionally robust neural networks for group shifts: On the importance of regularization for worst-case generalization. *arXiv preprint arXiv:1911.08731*, 2020. 2

Chitwan Saharia, William Chan, Saurabh Saxena, Lala Li, Jay Whang, Emily Denton, Seyed Kamyar Seyed Ghasemipour, Burcu Karagol Ayan, S. Sara Mahdavi, Rapha Gontijo Lopes, Tim Salimans, Jonathan Ho, David J Fleet, and Mohammad Norouzi. Photorealistic text-to-image diffusion models with deep language understanding. *arXiv preprint arXiv:2205.11487*, 2022. 1

Ramprasaath R. Selvaraju, Michael Cogswell, Abhishek Das, Ramakrishna Vedantam, Devi Parikh, and Dhruv Batra. Grad-cam: Visual explanations from deep networks via gradient-based localization. *arXiv preprint arXiv:1610.02391*, 2019. 3

Yang Song, Rui Shu, Nate Kushman, and Stefano Ermon. Constructing unrestricted adversarial examples with generative models. In *Advances in Neural Information Processing Systems*, 2018. 2

Andreas Steiner, Alexander Kolesnikov, Xiaohua Zhai, Ross Wightman, Jakob Uszkoreit, and Lucas Beyer. How to train your vit? data, augmentation, and regularization in vision transformers. *Transactions on Machine Learning Research*, 2022. 18

Christian Szegedy, Wojciech Zaremba, Ilya Sutskever, Joan Bruna, Dumitru Erhan, Ian Goodfellow, and Rob Fergus. Intriguing properties of neural networks. *arXiv preprint arXiv:1312.6199*, 2013. 2, 25

Christian Szegedy, Wei Liu, Yangqing Jia, Pierre Sermanet, Scott Reed, Dragomir Anguelov, Dumitru Erhan, Vincent Vanhoucke, and Andrew Rabinovich. Going deeper with convolutions. In *Proceedings of the IEEE/CVF Conference on Computer Vision and Pattern Recognition*, 2015. 18

Christian Szegedy, Sergey Ioffe, Vincent Vanhoucke, and Alexander A Alemi. Inception-v4, inception-resnet and the impact of residual connections on learning. In *Thirty-first AAAI conference on artificial intelligence*, 2017. 18

Antonio Torralba, Alexei A Efros, and others. Unbiased look at dataset bias. In *Proceedings of the IEEE/CVF Conference on Computer Vision and Pattern Recognition*, 2011. 1, 2

Sam Witteveen and Martin Andrews. Paraphrasing with large language models. *arXiv preprint arXiv:1911.09661*, 2019. 5

Eric Wong and J Zico Kolter. Learning perturbation sets for robust machine learning. In *International Conference on Learning Representations*, 2021. 2, 3

Chaowei Xiao, Bo Li, Jun-Yan Zhu, Warren He, Mingyan Liu, and Dawn Song. Generating adversarial examples with adversarial networks. *arXiv preprint arXiv:1801.02610*, 2018. 2

Kai Xiao, Logan Engstrom, Andrew Ilyas, and Aleksander Madry. Noise or Signal: The Role of Image Backgrounds in Object Recognition. *arXiv preprint arXiv:2006.09994*, 2020. 1, 2